JOURNAL OF GEOPHYSICAL RESEARCH, VOL. 112, B06423, doi:10.1029/2006JB004748, 2007

Effect of hydration state on the frictional properties of montmorillonite-based fault gouge

Matt J. Ikari,[1] Demian M. Saffer,[1] and Chris Marone[1]

Received 12 September 2006; revised 22 February 2007; accepted 27 March 2007; published 30 June 2007.

[1] We report on laboratory experiments examining the effect of hydration state on the frictional properties of simulated clay and quartz fault gouge. We tested four mixtures of Ca-montmorillonite and quartz (100, 70, 50, and 30% montmorillonite) at four hydration states: dry (<4.50 wt% water), one water interlayer equivalent (4.5–8.7 wt% water), two layers (8.7–16.0 wt% water), and three layer (>16.0 wt% water). We controlled the hydration state using either oven drying (for <13 wt% H_2O) or saline solutions (to achieve >13 wt% H_2O under conditions of controlled relative humidity). For each clay/quartz mixture and hydration state, we measured frictional properties over a range of normal stresses (5–100 MPa) and sliding velocities (1–300 μm/s). We observe a systematic decrease in the coefficient of friction (μ) with increasing water content, normal stress, and clay content. Values of μ for 50/50 mixtures range from 0.57 to 0.64 dry and decrease to 0.21–0.55 for the most hydrated cases (wet). For layers of 100% montmorillonite, μ ranges from 0.41–0.62 dry to 0.03–0.29 wet. As water content is increased from 0 to 20.0 wt%, the friction rate parameter a-b becomes increasingly positive. Variation in a-b values decreases dramatically as normal stress increases. If our experimental results can be applied to natural fault gouge, the combination of stress state, hydration state, and quartz content that facilitates unstable fault behavior implies that the onset of shallow seismicity in subduction zones is more complicated than a simple transition from smectite to illite.

Citation: Ikari, M. J., D. M. Saffer, and C. Marone (2007), Effect of hydration state on the frictional properties of montmorillonite-based fault gouge, *J. Geophys. Res.*, *112*, B06423, doi:10.1029/2006JB004748.

1. Introduction

[2] Understanding the frictional properties of fault gouge is crucial to understanding the generation and nature of earthquakes and the strength of crustal faults. For subduction zone faults, which form within fine-grained marine sediments, the expanding clay smectite is of particular interest because (1) it is common in the protolith [*Vrolijk and van der Pluijm*, 1999], (2) can exhibit exceptionally low friction [*Logan and Rauenzahn*, 1987; *Saffer et al.*, 2001], and (3) has been suggested as a candidate source of fault weakness [*Vrolijk*, 1990; *Morrow et al.*, 2000]. Water content of smectites is expected to decrease with depth due to increasing temperatures [*Bird*, 1984], and at temperatures of 100°–150°C, smectite transforms to illite [*Pytte and Reynolds*, 1989]. It has been observed that the onset of subduction zone seismicity coincides with this temperature range [*Hyndman et al.*,1997]. The clay mineral illite is frictionally stronger than smectite [*Morrow et al.*, 1992]; as such, it has been proposed that the updip limit of seismicity in subduction zones is controlled by the transformation of smectite to illite within the downgoing sediments [*Hyndman et al.*, 1997]. This theory has been called into question recently by studies indicating that while illite may be stronger than smectite, under sliding conditions, illite does not exhibit the unstable sliding behavior that would allow for seismogenesis [*Saffer and Marone*, 2003; *Kopf and Brown*, 2003; *Brown et al.*, 2003]. Although this indicates that the factors controlling the updip limit of seismicity may be more complicated than previously believed, water content may still be a major factor influencing the frictional behavior of subducting clays. Here we investigate the conditions that affect the strength of clay-dominated gouge, focusing on the mineral montmorillonite (a type of smectite) and quantifying the role of hydration state in strength and frictional behavior.

[3] Montmorillonite has been targeted as a potential source of fault weakness because of its unusually weak frictional behavior [*Vrolijk*, 1990]. It has been suggested that this weakness is the result of interstitial water within the clay structure [*Bird*, 1984; *Morrow et al.*, 2000]. We examined the effect of water on the frictional behavior of laboratory-simulated clay gouge by controlling its water content and by performing experiments in which we vary the normal stress, the shearing velocity, and the relative proportion of clay and quartz. Hydration state has been indirectly studied in previous work by controlling the ambient humidity on sealed layers consisting of 100%

[1]Department of Geosciences, Pennsylvania State University, University Park, Pennsylvania, USA.

0148-0227/07/2006JB004748$09.00

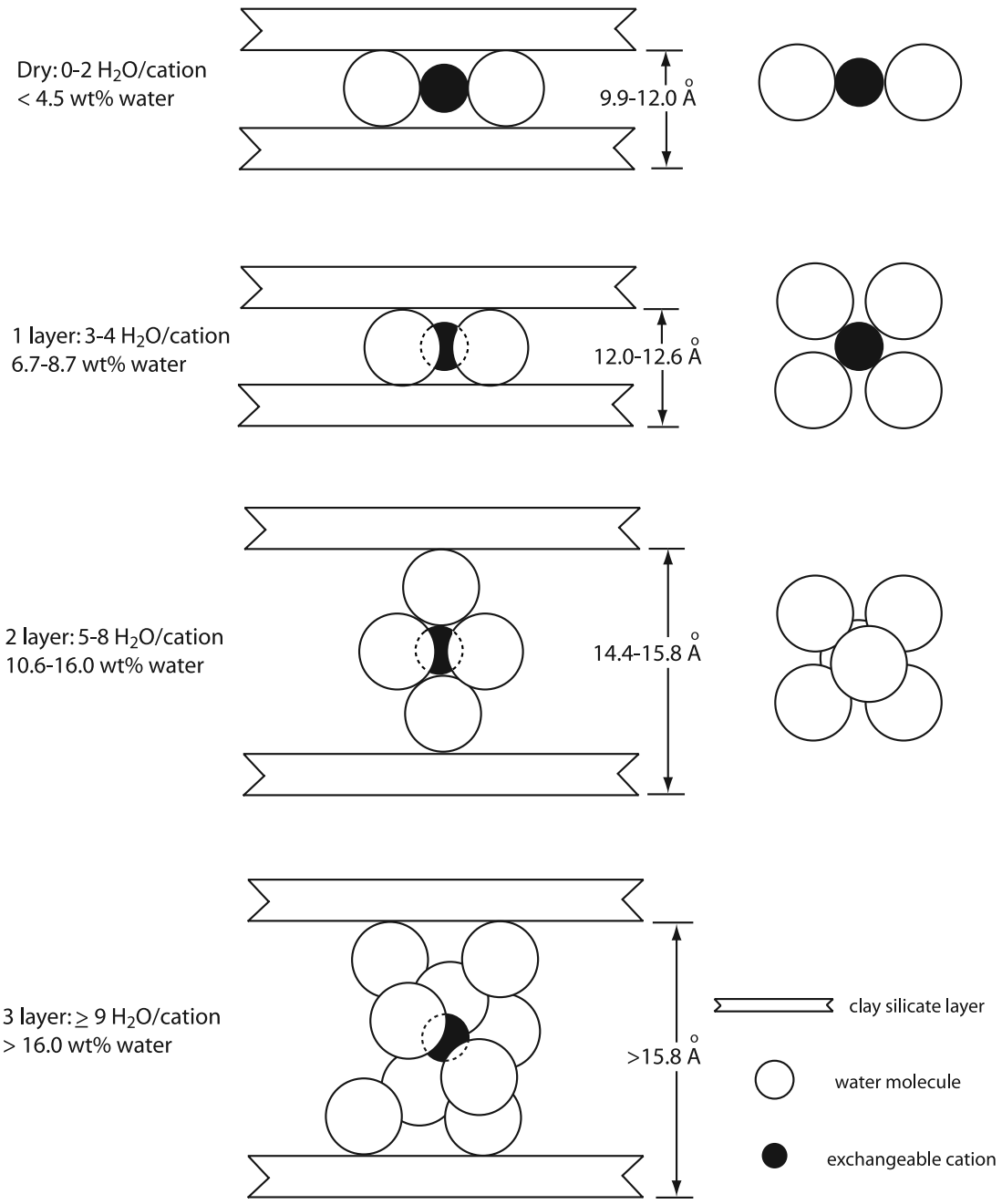

Figure 1. Structure of interlayer water in Ca-montmorillonite and corresponding weight percent. Dry layers contain fewer than two water molecules per cation. Two-layer arrangements are octahedral with six water molecules per cation. Above two layers, the water takes on a random arrangement. Note that intermediate hydration states may exist where more than one layer arrangement may be present. Modified from the work of *Colten-Bradley* [1987].

quartz [*Frye and Marone*, 2002], as well as some smectite-quartz mixtures at room conditions [*Saffer and Marone*, 2003; *Hong and Marone*, 2005]. The velocity-dependent frictional behavior of the quartz layers was found to change from strengthening to weakening with increasing relative humidity (RH). The overall frictional strength was unaffected by humidity [*Frye and Marone*, 2002]. Quartz, however, has a low capacity for water retention, so it is possible that the effect of water content is more pronounced in a layer either completely or partially composed of an expanding clay.

2. Experimental Methods

2.1. Water Content

[4] The aim of this study is to examine the effect of hydration state on frictional properties; therefore careful control of water content in the samples is essential. In previous experiments with layers consisting of 100% quartz,

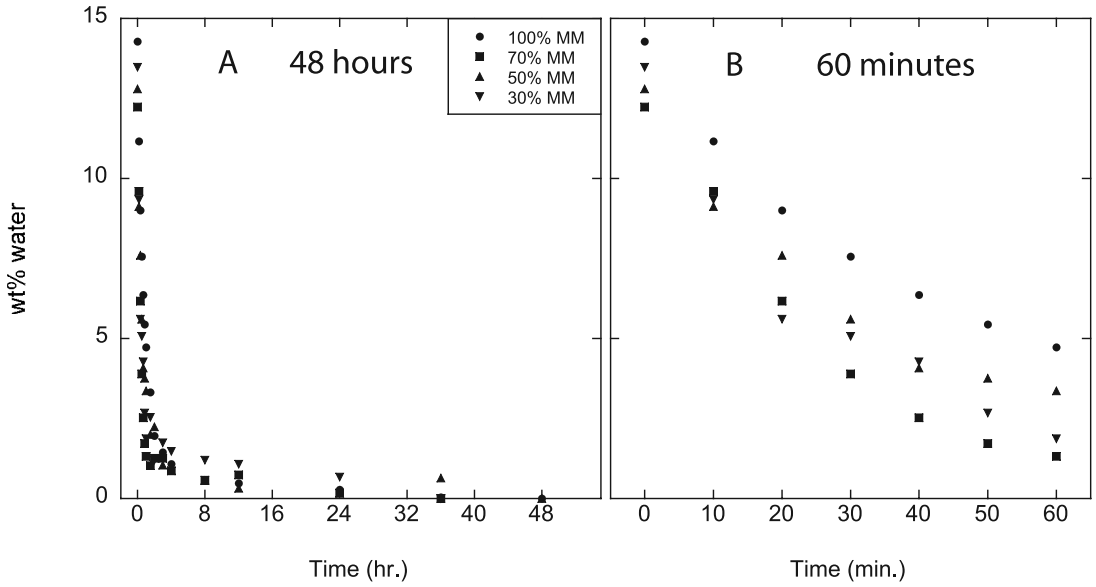

Figure 2. Experimentally derived time-dependent drying curve for all Ca-montmorillonite/quartz mixtures at 105°C for (a) 48 hours and (b) 60 min. MM = Ca-montmorillonite.

hydration state has been inferred by using a layer equilibrated with a controlled RH [*Frye and Marone*, 2002]. When montmorillonite reaches equilibrium with the surrounding air, the water content in the clay depends on the ambient temperature and RH [*Bird*, 1984]. Following the study of *Bird* [1984], we describe hydration state based on the number of water interlayers. These interlayer water molecules are bound to the silicate layers and the exchangeable cation, Ca^{2+}, in arrangements parallel to the silicate sheet (Figure 1). A one-layer arrangement includes three to four water molecules surrounding a cation, while a two-layer arrangement consists of six octahedrally bound water molecules [*Colten-Bradley*, 1987]. For clays in which water molecules are in excess of the two-layer arrangement (estimating a maximum of eight water molecules per cation), the water is oriented randomly similar to bulk water. We refer to this as a "three-layer" configuration. "Dry" samples are considered to be those containing less than three water molecules per cation. At room conditions (~45% RH and 25°C), montmorillonite contains water in a two-layer configuration [*Bird*, 1984].

[5] On the basis of a simple calculation using a molar mass of 757 g/mol for Ca-montmorillonite and 18 g/mol for water, we find that dry layers contain <4.5 wt% water, a one-layer arrangement contains 6.7–8.7 wt% water, a two-layer arrangement contains 10.6–16.0 wt% water, and a three-layer arrangement contains >16.0 wt% water (Figure 1). Samples may have intermediate water content; gouge that contains 9.2 wt% water, for example, may consist of clay particles with one and two water layers. To control the water content of our samples, we constructed time-dependent drying curves by dehydrating samples from room conditions via oven drying at 105°C and by recording the weight loss (Figure 2). The water content, or weight percent water, varies smoothly and predictably with time in response to heating. These data are highly reproducible and show that most water is driven off within the first 4 hours; although there is some variability between mixtures, any hydration state below ~13 wt% water can be attained. When no further weight reduction in the weight of clay sample was observed with continued heating, we designated this as the 0 wt% reference point in the drying curves. We verify that all bound water was driven off via oven drying by drying clay samples at elevated temperatures (~260°C) and by noting negligible further weight loss. Additionally, we performed Fourier-transform infrared spectroscopy (FTIR) on samples of oven-dried and room condition montmorillonite exposed to dry gas (nitrogen) for 210 min, results of which are consistent with a dry sample that is not more than ~1 wt% water and a room condition sample with ~13 wt% water. To reach water contents above that of a sample equilibrated with room humidity, we hydrated samples in a sealed environment containing a supersaturated Na_2CO_3 solution.

[6] Using the methods described above, we preconditioned simulated gouge material to a desired hydration state prior to each experiment (Table 1). During the experiments, the RH of the air surrounding the sample was controlled in a sealed environment to prevent any changes in water content. In addition, we verified that the hydration state at the end of each experiment was unchanged from the initial condition by oven drying the gouge immediately following the experiment.

[7] We conducted experiments in a biaxial testing apparatus to measure frictional behavior under controlled normal stress and sliding velocity. Two layers of sample fault gouge were sheared within a three-piece steel block assembly in a double-direct shear configuration (Figure 3). Gouge layers were constructed in a leveling jig to be uniform area (5 × 5 cm) and thickness (4–5 mm), which compacted to 2–3 mm under load. This three-block unit was then loaded into the testing apparatus, and a normal force was applied prior to shear (Figure 3). The frictional contact surfaces were grooved to ensure that shearing occurred within the layer and not at the layer-block interface. The contact area was maintained at 5 × 5 cm.

Table 1. Experiment Parameters[a]

Experiment	% Montmorillonite	σ_n, MPa	Layer Thickness Under Load, μm	wt% Water	Water Arrangement
p1019	70	15, 25, 40	3865	0.4	Dry
p699	50	5, 15, 24	3005	0.7	Dry
p696	30	5, 15, 40	3420	0.8	Dry
p706	70	5, 15, 24	3735	0.9	Dry
p787	30	5, 15, 26	3225	1.3	Dry
p709	100	40, 70, 100	2610	1.6	Dry
p788	30	40, 70, 99	2945	1.7	Dry
p1018	100	5, 15	4215	1.7	Dry
p790	50	40, 70, 99	3290	2.3	Dry
p736	30	5, 15, 24	3505	2.4	Dry
p695	30	40, 70	2840	2.5	Dry
p701	70	40, 70, 100	3100	2.6	Dry
p711	100	5, 15, 24	3640	2.6	Dry
p735	30	5, 15, 24	–	3.3	Dry
p740	50	40, 70, 100	3285	4.5	One-layer
p733	50	6, 15	2380	5.8	One-layer
p748	50	40, 70, 100	3155	6.7	One-layer
p747	50	5, 15, 25	2990	6.8	One-layer
p738	100	40, 70, 100	2510	6.9	One-layer
p784	50	5, 15, 24	3105	7.2	One-layer
p723	100	5, 15, 24	3825	7.3	One-layer
p730	70	5, 15, 24	3960	7.5	One-layer
p749	70	40, 70, 100	3045	7.7	One-layer
p751	30	5, 15, 24	3385	7.9	One-layer
p752	30	40, 70, 100	2625	7.9	One-layer
p1012	50	5, 15, 26	4220	8.2	One-layer
p1011	100	5, 15	3450	8.7	One-layer
p783	70	5, 15, 25	3750	8.9	Two-layer
p846	70	40, 70, 99	3070	9.0	Two-layer
p775	70	40, 70, 99	3040	10.6	Two-layer
p782	70	40, 70, 99	2945	11.6	Two-layer
p1037	50	40, 70, 99	3310	11.8	Two-layer
p1007	100(<45 μm)	5, 15, 25	3405	12.6	Two-layer
p780	30	5, 15, 25	3340	12.9	Two-layer
p781	30	40, 70, 100	2765	13.1	Two-layer
p1008	100(<45 μm)	40, 70, 99	2290	13.3	Two-layer
p776	100	5, 15, 24	3310	13.7	Two-layer
p774	100	40, 70, 100	2620	13.7	Two-layer
p777	50	5, 15, 25	3045	13.9	Two-layer
p759	70	5, 15, 24	3860	14.5	Two-layer
p734	50	5, 15, 24	3200	14.9	Two-layer
p807	100	5, 15, 24	3410	17.0	Three-layer
p806	100	40, 70, 100	2485	17.1	Three-layer
p805	70	41, 71, 101	2605	17.2	Three-layer
p808	50	5, 15, 25	3780	17.5	Three-layer
p809	50	40, 70, 99	2975	17.5	Three-layer
p815	30	5, 15, 25	3290	17.9	Three-layer
p816	30	40, 70, 99	2555	18.2	Three-layer
p849	100	40, 70, 99	2155	19.4	Three-layer
p814	70	5, 15, 25	3410	19.5	Three-layer
p858	100	5, 15, 25	3130	20.0	Three-layer
p859	100 (Na) (3 μm)	5, 15, 25	3290	0.5	Dry
p861	100 (Na) (3 μm)	40, 70, 100	2530	0.5	Dry
p857	100 (Na) (3 μm)	5, 15, 25	3575	5.5	One-layer
p850	100 (Na) (3 μm)	40, 70, 99	1950	5.6	One-layer
p886	100 (Na) (3 μm)	40, 70, 99	2165	12.1	Two-layer
p874	100 (Na) (3 μm)	4, 14, 24	2930	13.0	Two-layer

[a]Parameters for the suite of experiments. Clay is Ca-montmorillonite unless specified as Na. Mean grain size is 60 μm unless specified. Layer thickness under load taken at the lowest normal stress in experiment.

[8] We ran a suite of experiments at normal stresses ranging from 5 to 100 MPa for a series of gouge compositions (ranging from 0 to 70% quartz by weight) and for a range of controlled hydration states (Table 1). Mean grain size of Ca-montmorillonite was 60 μm, with 80% of the grain diameters between 3 and 142 μm, determined by using laser obscuration in a Malvern Mastersizer. Mean grain size of quartz sand was 110 μm; grain sizes fit a Gaussian distribution, with 99% of the grain diameters between 53 and 212 μm.

[9] Measurements of initial porosity were made by dividing the void volume (total volume minus sediment volume) by the total volume of the sample following the work of *Marion et al.* [1992]. Total volume was the contact area times the initial layer thickness; sediment volume was the mass of gouge material divided by the sample density.

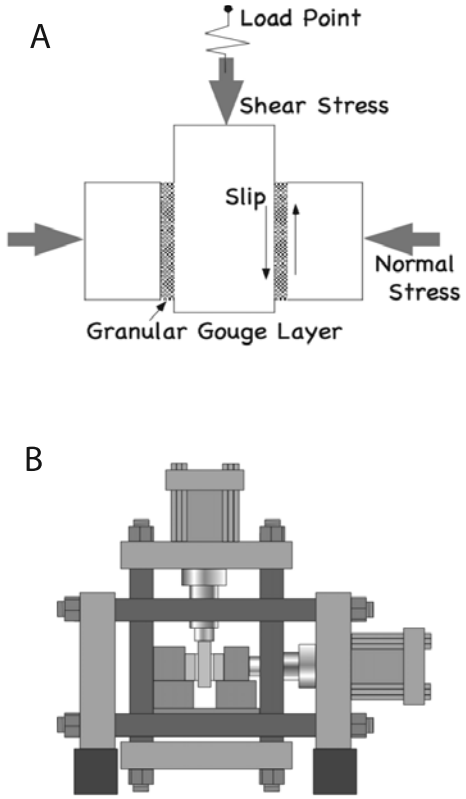

Figure 3. (a) Setup of biaxial stress experiments. Samples are loaded in-between grooved sliding blocks. (b) Sliding blocks are then loaded in biaxial stressing apparatus.

Sample density varied between 2.35 and 2.78 g/cm^3 depending on the clay percentage and water content of the clay portion [*Lambe and Whitman*, 1969]. The initial porosity of samples (on the benchtop, under a load of ~6 kPa) composed of 30% montmorillonite was 50% for dry samples and 46% for three-layer samples. Porosity of 100% montmorillonite was 61% for dry samples and 58% for three-layer samples. Initial porosity values for samples with two water interlayers are 44, 48, 51, and 54% in samples composed of 30, 50, 70, and 100% montmorillonite, respectively. The values we report are similar to porosity values obtained by *Marion et al.* [1992] at atmospheric conditions.

[10] Gouge layers were sheared at constant velocity for the first 10 mm of fault slip to develop a steady state fabric and to minimize any effect of net displacement. Three sets of velocity step sequences were then initiated, each of them being at a given normal stress (Table 1, Figure 4). Each velocity step sequence consisted of incrementally increasing the sliding velocity from 1 to 300 μm/s and then back down to 10 μm/s. The duration of each velocity step was the time necessary to displace a distance of 400 μm. Steady state sliding was usually achieved after ~1.5 mm of displacement in each sequence. We measured overall shear strength of fault gouge (τ) and coefficient of sliding friction (μ) after 10 mm of displacement after application of each normal stress for consistency (Figure 4). The coefficient of sliding friction μ was calculated as: $\tau = \mu\sigma_n + c$, where σ_n is the applied normal stress [*Handin*, 1969; *Byerlee*, 1978] and the intercept c is the cohesion (typically zero for our experimental gouge).

3. Results

3.1. Frictional Strength

[11] The shear strength (and coefficient of friction) of the gouge is strongly dependent on its water content (Figures 5 and 6). This effect is more pronounced with increased

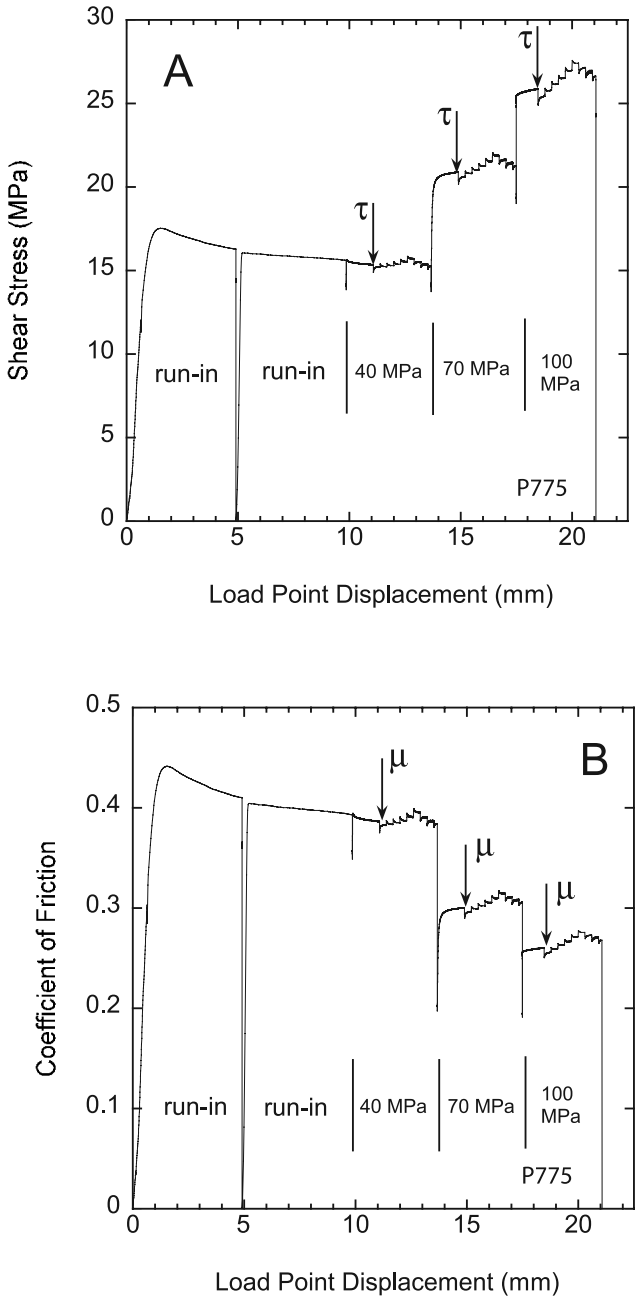

Figure 4. Example of a typical experiment: (a) Shear stress and (b) coefficient of friction are plotted against load point displacement, which is equal to the displacement during sample shearing. The shear strength value τ and the coefficient of friction μ are taken after 1.6 mm of displacement during each velocity step sequence.

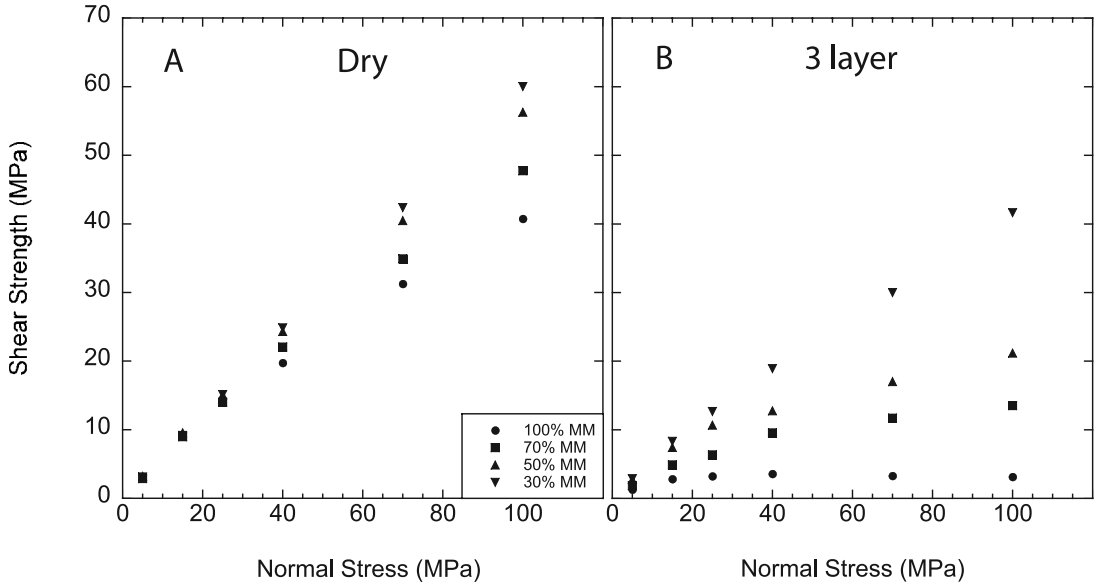

Figure 5. Shear strength with increasing normal stress for all mixtures, comparing (a) the most dry samples and (b) the most hydrated three-layer samples.

normal stress and with higher clay content (Figure 5). The failure envelope exhibits rollover at 25–40 MPa; this is more dramatic with increased clay and increased water content (Figure 5). The steady state coefficient of sliding friction decreases systematically with increasing water content, normal stress, and clay content (Figures 6 and 7). For example, at 40 MPa, μ ranges from 0.49 and 0.62 dry, while three-layer samples range from 0.09 to 0.48 for all mixtures. With water content held constant, increased normal stress also reduces the coefficient of friction for all mixtures; for example, in the one-layer samples, μ decreases from 0.52–0.64 at 5 MPa to 0.23–0.56 at 100 MPa. Note that the reduction in μ is more pronounced in layers with higher clay percentage; in comparing mixtures containing 30 and 100% montmorillonite over all normal stresses and hydration states, both mixtures have similar maximum values (0.62 for 100% and 0.63 for 30%), but μ in 100% montmorillonite decreases to 0.03 at high normal stress and water content while the minimum value of μ for 30% montmorillonite layers under the same conditions is 0.42. This is consistent with previous findings in which increased clay percentage causes a decrease in coefficient of friction [*Logan and Rauenzahn*, 1987].

3.2. Velocity Dependence

[12] We classify frictional velocity dependence using the parameter a-b defined as $(a-b) = \frac{\Delta\mu_{ss}}{\ln(V/V_o)}$, where $\Delta\mu_{ss}$ is the change in steady state sliding friction, and V_o and V are

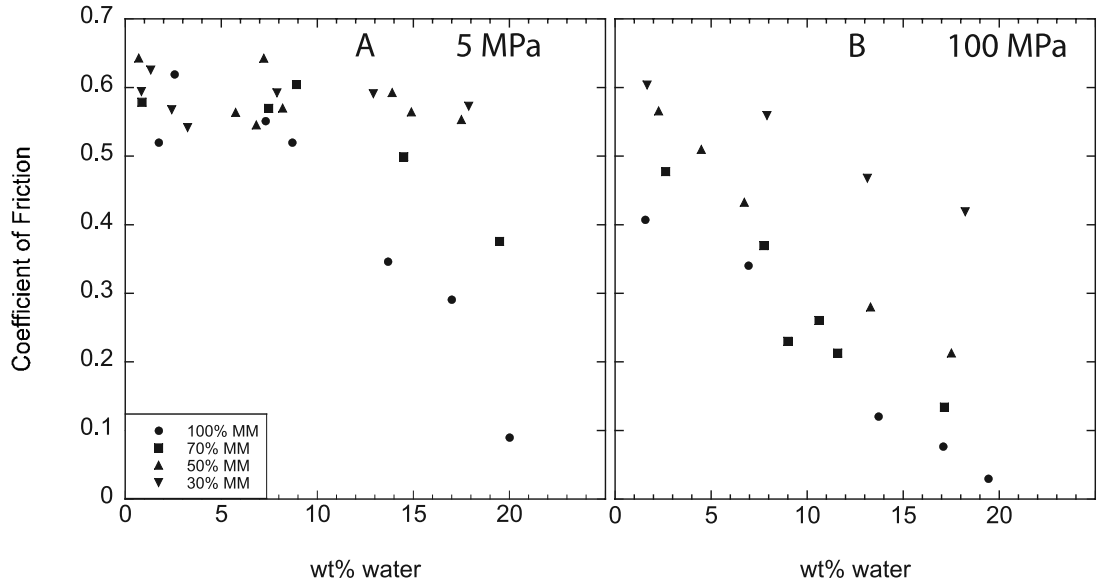

Figure 6. Coefficient of friction plotted against increasing water content at normal stresses of (a) 5 MPa and (b) 100 MPa.

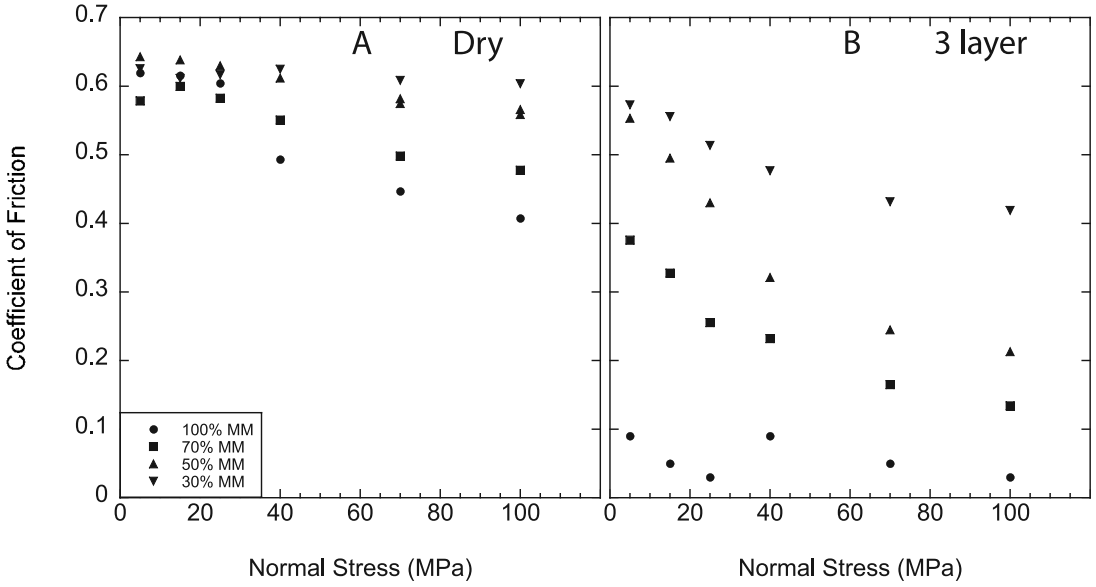

Figure 7. Coefficient of friction plotted against increasing normal stress, showing all mixtures and comparing (a) the driest samples with (b) the most hydrated three-layer samples.

the sliding velocities at initial and new steady state friction, respectively [e.g., *Marone*, 1998], (Figure 8). Positive *a-b* values indicate velocity-strengthening behavior, whereas negative *a-b* values indicate velocity-weakening behavior. Velocity weakening is a prerequisite for stick-slip behavior which is associated with earthquake nucleation [*Scholz*, 2002].

[13] Results of the velocity stepping tests indicate that the majority of the gouge samples exhibit velocity-strengthening behavior. For all mixtures, we observe a large variance in *a-b* for low normal stress and variance decreases with increased normal stress. Dry samples, as opposed to samples with at least one layer of bound water, maintain some velocity-weakening behavior throughout the entire normal stress regime (whereas the hydrated samples do not) and are less velocity strengthening in general (Figure 9). At 5 MPa, both hydrated and dry samples have similarly large ranges of *a-b* (-0.0042 to 0.0123 for hydrated samples and -0.0037 to 0.0140 for dry samples), whereas at 100 MPa, the *a-b* values in hydrated layers range from 0.0005 to 0.0049 and, in dry layers, values range from -0.0008 to 0.0020.

[14] In hydrated samples, the lowest values of *a-b* are associated with low sliding velocity (1–3 μm/s); these change from velocity weakening to velocity strengthening with increased normal stress, which is consistent with previous data [*Saffer et al.*, 2001], (Figure 10). The more positive *a-b* values are associated with samples sliding at high velocity (100–300 μm/s); these tend to decrease with increased normal stress. The same trend can be identified in

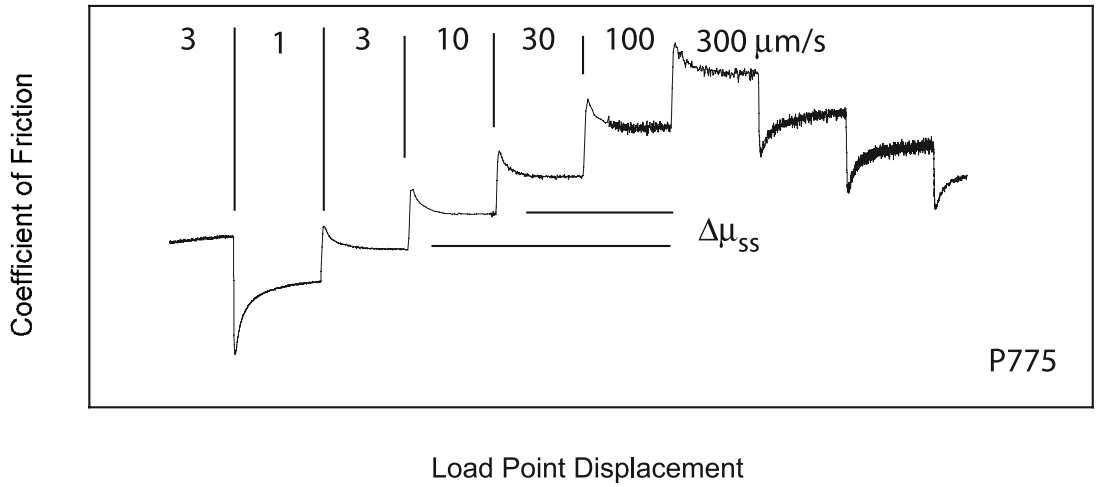

Figure 8. An example of a velocity step sequence and the change in steady state sliding friction used to determine the parameter *a-b*. Sliding velocity is instantaneously increased, and *a-b* is calculated using the value of $\Delta\mu_{ss}$ as a result of the increase.

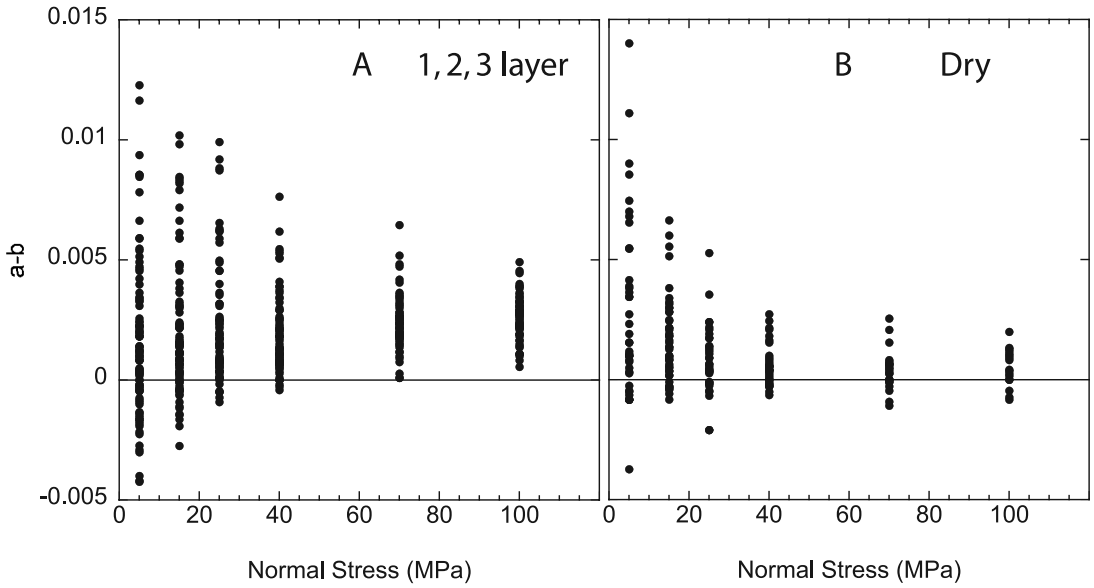

Figure 9. *a-b* values for all mixtures with increasing applied normal stress for (a) one-, two-, and three-layer samples (>4.5 wt% water) and (b) dry samples (<4.5 wt% water).

dry samples but is less clearly defined than in the hydrated samples. Generally, at a given normal stress, higher sliding velocity yields more positive *a-b* values (Figure 11).

[15] With increased sliding velocity, two additional trends can be identified. First, samples with higher clay percentage are generally more velocity strengthening regardless of water content (Figure 12). Second, within the trend in *a-b* for each individual gouge mixture, higher water content slightly increases *a-b* values. In the most hydrated samples, those containing 30% montmorillonite are comparable only to the lowest *a-b* values exhibited by 100% montmorillonite regardless of normal stress and sliding velocity (Figure 12). In dry samples, *a-b* values are comparable, but it is noteworthy that mixtures containing 30% montmorillonite show velocity-weakening behavior for all normal stresses.

3.3. Na-Montmorillonite

[16] We performed six experiments with 100% Na-montmorillonite in order to determine whether frictional behavior is cation-specific. These experiments yielded data for dry (0.5 wt% water), one-layer (5.5, 5.6 wt% water), and two-layer (12.1, 13.0 wt% water) samples over the same range of normal stresses and sliding velocities as the Ca-montmorillonite experiments (Table 1). Room condition Na-montmorillonite samples were one-layer, and hydrated samples were two-layer, lower states of hydration than Ca-montmorillonite at the same conditions. This is expected because the lower charge of Na^+ doubles the negative charge of the clay structure, allowing approximately half the amount of water to remain in the interlayer [*Eberl et al.*, 1993]. Sliding friction values for Na-montmorillonite are 0.55 to 0.45 for dry samples, 0.35 to 0.22 for one-layer

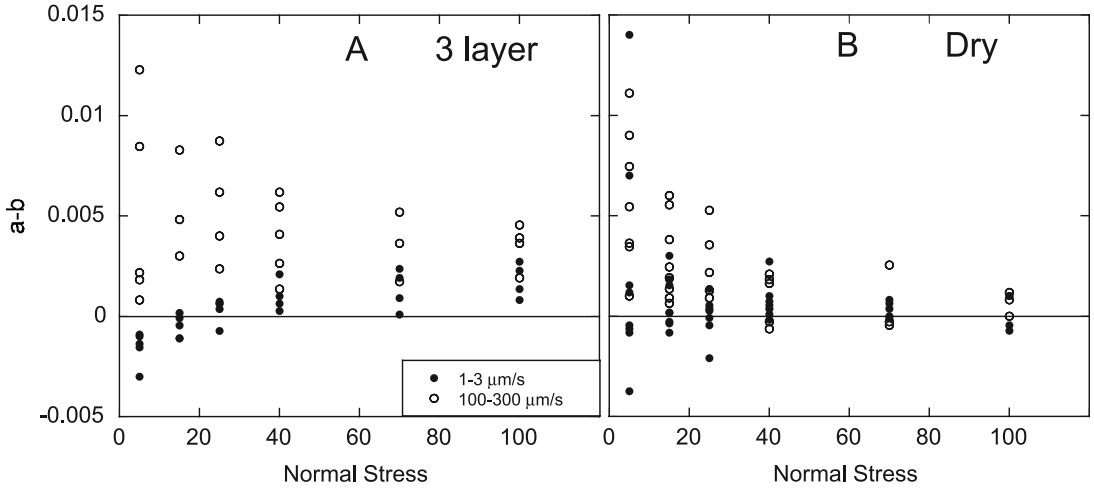

Figure 10. *a-b* for all mixtures with increasing normal stress, comparing high and low sliding velocities for (a) three-layer and (b) dry samples.

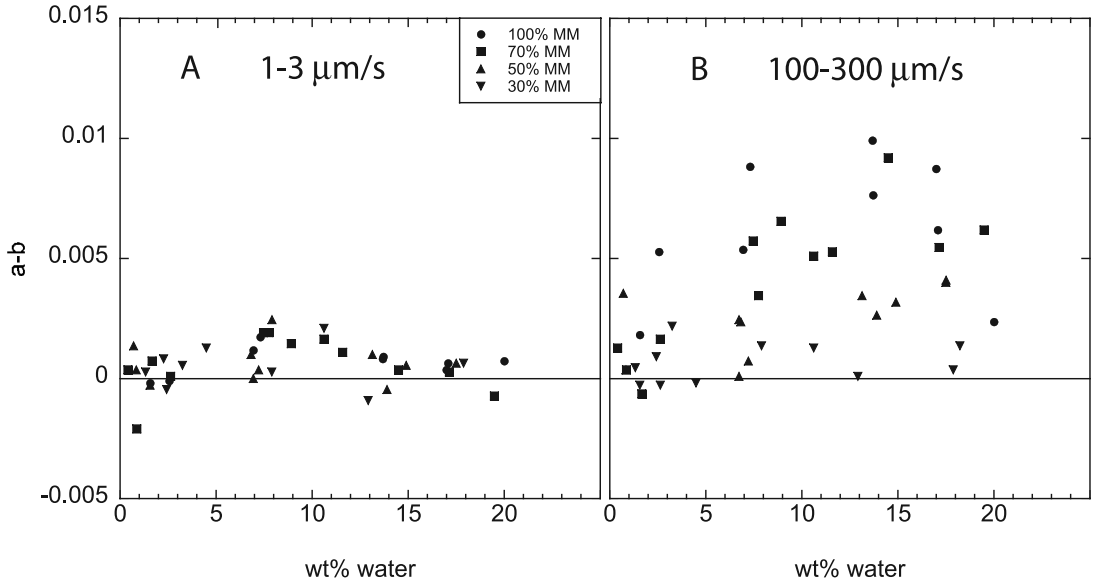

Figure 11. *a-b* plotted against increasing water content for all mixtures at a normal stress of 25 MPa, comparing (a) sliding velocity increase from 1 to 3 μm/s and (b) sliding velocity increase from 100 to 300 μm/s.

samples, and 0.28 to 0.04 for two-layer samples. Compared to Ca-montmorillonite, values of μ for dry samples are slightly lower ($\sim$0.05 lower), and one-layer and two-layer values are significantly lower ($\sim$0.1 to 0.15 lower for all normal stresses). However, the trend of lower friction values with both increasing water content and increasing normal stress remains the same as for Ca-montmorillonite. Observations of frictional velocity dependence for Na-montmorillonite are also consistent with those for Ca-montmorillonite.

4. Discussion

4.1. Comparison to Previous Data

[17] The trends in μ we observe are in very good agreement with previous work conducted on montmorillonite gouge. For two-layer 100% montmorillonite, μ decreases from 0.35 to 0.12 as normal stress is increased from 5 to 100 MPa, and for two-layer samples containing 50% montmorillonite, μ decreases from 0.59 to 0.27 over the same normal stress range. This is comparable to the results of *Saffer and Marone* [2003] in which μ decreased from $\sim$0.32 to $\sim$0.10 and from $\sim$0.57 to $\sim$0.21 in layers of 100 and 50% montmorillonite, respectively, under the same normal stress range. The large decrease in μ from 0.60 under dry conditions to 0.03 in three-layer 100% montmorillonite at 25 MPa is similar to the decrease observed by *Morrow et al.* [1992] when comparing dry and saturated montmorillonite gouge. At 40 and 70 MPa, values of μ for three-layer 30, 70, and 100% montmorillonite samples are similar to values reported by *Logan and Rauenzahn* [1987] at 50- and 70-MPa confining pressure for 25, 75, and 100%

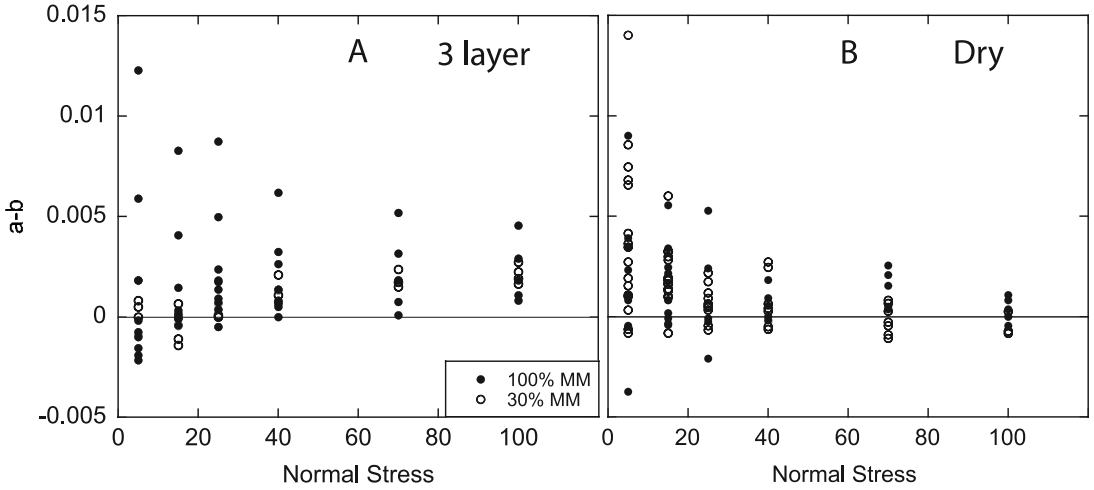

Figure 12. *a-b* values with increasing normal stress, comparing high clay percentage (100% MM) and low clay percentage (30% MM) for (a) three-layer and (b) dry samples.

montmorillonite samples. We also observe systematically higher values of μ in samples with higher quartz content; this was also observed by *Logan and Rauenzahn* [1987] and *Kopf and Brown* [2003] who document a strong correlation between increasing μ and decreasing clay content (increasing quartz content).

[18] The systematic increase in μ with increasing quartz content may also be related to the strength of grain-to-grain contacts between minerals [*Logan and Rauenzahn*, 1987]. We observe that gouge samples with higher quartz content have lower initial porosity values than samples with high clay content. However, when subjected to normal stress prior to shearing, the high quartz samples tend to have higher porosities. We infer that once a normal load has been applied, the major mineralogic constituent in the gouge supports the majority of the load; i.e., in gouge with high quartz content, quartz grains will likely impinge on other quartz grains, and in gouge with high clay content, the clay minerals will likely impinge on each other [*Marion et al.*, 1992]. Thus the shear strength of the gouge will be controlled by the strength of the minerals in contact with each other rather than the initial porosity. Quartz strength is independent of humidity, with $\mu = \sim 0.6-0.65$ [*Mair and Marone*, 1999; *Frye and Marone*, 2002], whereas we observe that montmorillonite strength is highly variable and is inversely related to water content.

[19] Although the trend of weakening with increasing water content in montmorillonite is clear, the mechanism by which this weakening occurs is not. A variety of mechanisms have been suggested for water-assisted weakening of fault gouge. Expulsion of interlayer water from a bound state within the crystal structure to pore space due to mechanical pressure may reduce friction by increasing the pore pressure, thereby reducing the effective normal stress [e.g., *Colten-Bradley*, 1987; *Fitts and Brown*, 1999]. In a compaction experiment in which two-layer 100% montmorillonite was subjected to load steps of 5, 15, 25, 40, 70, and 100 MPa for a duration of 15 min without shearing, porosity was reduced from 59% under zero normal load to 7% at 100 MPa. This indicates that porosity reduction due to compaction and shear could potentially have brought the porosity to extremely low values. Because we performed experiments on undersaturated sediments, expulsion of bound water from the clay structure may not significantly affect the sample porosity, as bound water expulsion into pore space is approximately compensated by pore volume increase due to collapse of the clay mineral structure once the water is expelled. Nevertheless, the porosity may have been reduced enough that transient pore pressure buildup may have occurred.

[20] Another potential explanation is that interlayer water may support the applied normal stress within the clay structure itself, thereby allowing slip at low effective stress between the octahedral layers [*Bird*, 1984]. At the moment, however, there is little evidence that this particular mechanism occurs. In contrast to experiments on undersaturated sediments, several previous studies report on friction experiments with sediments saturated with deionized water [*Moore and Lockner*, 2004; *Moore and Lockner*, 2007] or brine having seawater composition [*Brown et al.*, 2003; *Kopf and Brown*, 2003]. Some of these studies suggest that low friction values represent the strength necessary to shear through films of water molecules bonded to mineral surfaces in proportion to that mineral's interlayer charge [*Moore and Lockner*, 2004; *Moore and Lockner*, 2007]. Although the composition of the pore fluid may increase the strength of montmorillonite gouge, this increase is very small (0.02 increase in μ in the presence of a 1-M brine) [*Lockner et al.*, 2006]. It may be possible that these surface effects due to saturation, and effective stress changes caused by increased pore pressure, combine to cause unusually weak gouge. More experimentation is necessary to determine the exact mechanism of gouge weakening.

[21] Our observed trends in *a-b* are also in close agreement with previous studies. Most of the previous studies have been conducted on samples sheared to very limited displacements and without precise control on sample normal stress, which tends to result in biased results for friction velocity dependence [e.g., *Dieterich*, 1981; *Beeler et al.*, 1996]. However, we compare to those values for completeness. *Morrow et al.* [1992] report an *a-b* value of 0.0005 for 100% montmorillonite at 100 MPa, which is consistent with our data. *Logan and Rauenzahn* [1987] report that 100% quartz is velocity weakening, while all other clay mixtures in their study were velocity strengthening. Because their samples were not oven-dried, this observation is most comparable to our reported *a-b* values for partially hydrated samples. *Logan and Rauenzahn* [1987] and *Saffer et al.* [2001] also observed unstable sliding at very low velocity. We also observe this behavior; however, at higher sliding velocities and higher normal stress, this behavior vanishes in all but the dry samples, which is consistent with previous observations of velocity strengthening behavior in nondry mixtures containing montmorillonite [*Logan and Rauenzahn*, 1987; *Saffer et al.*, 2001]. The similarity of these observations leads to two important points. First, the presence of (nondry) montmorillonite causes fault gouge to be weak; progressive increase in relative quartz percentage causes the gouge to strengthen. Second, other than some unstable behavior at very low sliding velocity and very low normal stress, montmorillonite gouge slides stably even in very low proportions (30%), whereas quartz exhibits unstable sliding.

4.2. Application to Natural Systems

[22] We have shown the systematics of the frictional behavior of montmorillonite-quartz gouges over a wide range of conditions, including water content, applied normal stress, clay content, and sliding velocity. Realistically, however, the range of these conditions in natural faults is much narrower. For example, subduction zones do not consist of 100% Ca-montmorillonite nor does clay retain 20 wt% water to depths at which pressures are 100 MPa. To apply our experimental results to subduction zone conditions, we must consider a subset of our experiments that are consistent with in situ fault gouge compositions and hydration states.

[23] We may estimate the conditions of hydration and bulk clay content with depth. For real faults, we assume an effective vertical component of normal stress increase of 8 MPa/km and a temperature gradient of 20–25°C/km. Water content decreases with increasing depth; with effective stresses as low as ~1.3 MPa, smectite may not contain more than two layers of water [*Fitts and Brown*, 1999].

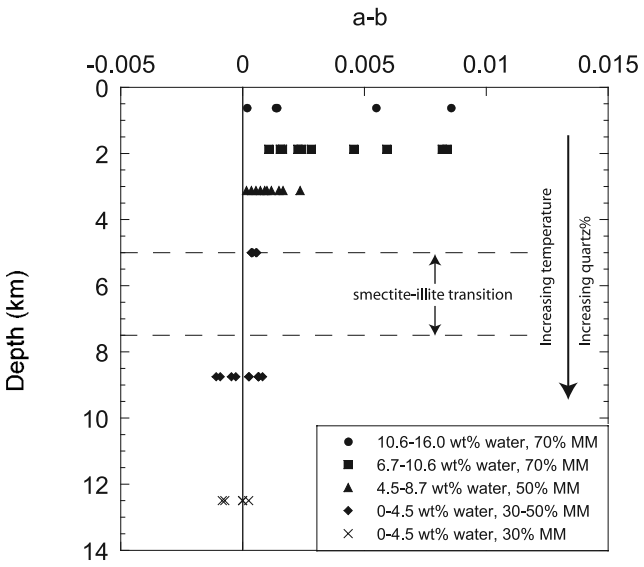

Figure 13. *a-b* values at conditions that may be expected at given depths in a subduction zone. Assumed effective pressure gradient is 8 MPa/km and assumed temperature gradient is 20°–25°C/km.

Because of increasing temperature and normal stress, interlayer water content reduces to one layer at 67°–81°C, and the remaining layer is expelled at 172°–192°C [*Colten-Bradley*, 1987]. This corresponds to clay containing one layer of water at ~3–8 km; and at depths greater than 8 km, only "dry" clay may exist. Although abundant fluid and overpressures may exist within fault zones, the thermally driven expulsion of interlayer water should result in "dry" montmorillonite, with fluid being in pore spaces rather than in the clay interlayers [*Colten-Bradley*, 1987].

[24] Smectite content in gouge can be large [*Vrolijk and van der Pluijm*, 1999]; at many subduction zones, for example, the percentage of smectite in the bulk sediment can be greater than 50% [*Underwood*, 2007]. Above 150°C (and below 300°C), significant quartz precipitation may occur via pressure solution and recrystallization downdip, increasing the relative percentage of quartz [*Moore and Saffer*, 2001; *Moore et al.*, 2006]. In applying our data to natural faults, we assume an initial gouge composition of 70% montmorillonite which changes gradually to 30% montmorillonite with depth. Given that quartz is velocity weakening in this pressure and temperature window [*Blanpied et al.*, 1998; *Mair and Marone*, 1999], we expect the gouge to become more velocity weakening as the relative percentage of quartz to stably sliding clay (which by this depth has most likely been transformed to illite) increases with depth.

[25] In a simplified analysis merging our data with estimated in situ subduction zone conditions and progressive changes in gouge compositions, we see clear velocity-weakening trend and crossover into negative *a-b* values between 5 and 9 km depth, consistent with both the updip limit of seismicity and the smectite-illite transition (Figure 13). The data are shown here without regard for sliding velocity; however, recall from Figure 11 that high sliding velocities tend to accentuate the trend toward velocity strengthening. This result suggests that although the updip limit of seismicity may coincide with the smectite-illite transition temperature, this transition alone may not be sufficient to cause fault gouge to become seismogenic. Instead, it appears that the onset of seismic behavior is more complicated and requires a combination of conditions that include, but may not be limited to, quartz content, clay dehydration, sliding velocity, and stress state. More experimentation is necessary to conclusively determine the relative importance of these and other factors.

5. Conclusions

[26] Water content of montmorillonite has a profound effect on the frictional strength and constitutive properties of fault gouge. With increasing water content, the overall frictional strength of gouge becomes much lower and, in the cases of very high water and clay content, gouge exhibits rollover in the frictional failure envelope (i.e., above a given normal stress, shear strength increases only slightly). Increasing water content also leads to velocity-strengthening behavior. In applying our results to the geologic conditions in subduction zones, we note that decreasing water content, increasing quartz content, and increasing normal stress may combine to cause a transition to velocity-weakening behavior at depths consistent with the onset of subduction zone seismicity. The smectite-illite transition by itself does not appear to be sufficient to explain the onset of subduction zone seismicity.

[27] **Acknowledgments.** This paper benefited from discussions with Lee Kump and Peter Heaney. We thank Doug Archibald for the FTIR work. We are grateful to Ernie Rutter, Achim Kopf, and John Logan for their reviews and for providing helpful suggestions to improve this paper. This work was supported by National Science Foundation grants EAR-0196570, OCE-0196462, and EAR-0337627.

References

Beeler, N. M., T. E. Tullis, M. L. Blanpied, and J. D. Weeks (1996), Frictional behavior of large displacement experimental faults, *J. Geophys. Res.*, *101*, 8697–8715.

Bird, P. (1984), Hydration-phase diagrams and friction of montmorillonite under laboratory and geologic conditions, with implications for shale compaction, slope stability, and strength of fault gouge, *Tectonophysics*, *107*, 235–260.

Blanpied, M. L., C. Marone, D. A. Lockner, J. D. Byerlee, and D. P. King (1998), Quantitative measure of the variation in fault rheology due to fluid-rock interactions, *J. Geophys. Res.*, *103*, 9691–9712.

Brown, K. M., A. Kopf, M. B. Underwood, and J. L. Weinberger (2003), Compositional and fluid pressure controls on the state of stress on the Nankai subduction thrust: A weak plate boundary, *Earth Planet. Sci. Lett.*, *214*, 589–603.

Byerlee, J. D. (1978), Friction of rocks, *Pure Appl. Geophys.*, *116*, 215–626.

Colten-Bradley, V. A. (1987), Role of pressure in smectite dehydration—Effects on geopressure and smectite-to-illite transformation, *AAPG Bull.*, *71*, 1414–1427.

Dieterich, J. D. (1981), Constitutive properties of faults with simulated gouge, in *Mechanical Behavior of Crustal Rocks (The Handin Volume)*, *Geophys. Monogr. Ser.* vol. 24, edited by N. L. Carter et al., pp. 103–120, AGU, Washington, D. C.

Eberl, D. D., B. Velde, and T. McCormick (1993), Synthesis of illite-smectite from smectite at earth surface temperatures and high pH, *Clay Miner.*, *28*, 49–60.

Fitts, T. G., and K. M. Brown (1999), Stress-induced smectite dehydration: Ramifications for patterns of freshening and fluid expulsion in the N. Barbados accretionary wedge, *Earth Planet. Sci. Lett.*, *172*, 179–197.

Frye, K. M., and C. Marone (2002), Effect of humidity on granular friction at room temperature, *J. Geophys. Res.*, *107*(B11), 2309, doi:10.1029/2001JB000654.

Handin, J. (1969), On the Coulomb-Mohr failure criterion, *J. Geophys. Res.*, *74*, 5343–5348.

Hong, T., and C. Marone (2005), Effects of normal stress perturbations on the frictional properties of simulated faults, *Geochem. Geophys. Geosyst.*, *6*, Q03012, doi:10.1029/2004GC000821.

Hyndman, R. D., M. Yamano, and D. A. Oleskevich (1997), The seismogenic zone of subduction thrust faults, *Isl. Arc*, *6*, 244–260.

Kopf, A., and K. M. Brown (2003), Friction experiments on saturated sediments and their implications for the stress state of the Nankai and Barbados subduction thrusts, *Mar. Geol.*, *202*, 193–210.

Lambe, T. W., and R. V. Whitman (1969), *Soil Mechanics*, John Wiley, Hoboken, N. J.

Lockner, D., J. Solum, and N. Davatzes (2006), The effect of brine composition and concentration on strength of expandable clays, *Eos Trans. AGU*, *87*(52), Fall Meet. Suppl., Abstract T31F-03.

Logan, J. M., and K. A. Rauenzahn (1987), Frictional dependence of gouge mixtures of quartz and montmorillonite on velocity, composition, and fabric, *Tectonophysics*, *144*, 87–108.

Mair, K., and C. Marone (1999), Friction of simulated fault gouge for a wide range of velocities and normal stresses, *J. Geophys. Res.*, *104*, 28,899–28,914.

Marion, D., A. Nur, H. Yin, and D. Han (1992), Compressional velocity and porosity in sand-clay mixtures, *Geophysics*, *57*, 554–563.

Marone, C. (1998), Laboratory-derived friction laws and their application to seismic faulting, *Annu. Rev. Earth Planet. Sci.*, *26*, 643–696.

Moore, D. E., and D. A. Lockner (2004), Crystallographic controls on the frictional behavior of dry and water-saturated sheet structure minerals, *J. Geophys. Res.*, *109*, B03401, doi:10.1029/2003JB002582.

Moore, D. E., and D. A. Lockner (2007), Friction of the smectite clay montmorillonite: A review and interpretation of data, in *The Seismogenic Zone of Subduction Thrust Faults*, edited by T. Dixon et al., Columbia Univ. Press, New York.

Moore, J .C., and D. M. Saffer (2001), Updip limit of the seismogenic zone beneath the accretionary prism of Southwest Japan: An effect of diagenetic to low-grade metamorphic processes and increasing effective stress, *Geology*, *29*, 183–186.

Moore, J. C., C. Rowe, and F. Meneghini (2006), How accretionary prisms elucidate seismogenesis in subduction zones, in *Interplate Subduction Zone Seismogenesis*, edited by J. C. Moore and T. H. Dixon, Columbia Univ. Press, New York.

Morrow, C., B. Radney, and J. Byerlee (1992), Frictional strength and the effective pressure law of montmorillonite and illite clays, in *Fault Mechanics and Transport Properties of Rocks*, edited by B. Evans and T. F. Wong, pp. 69–88, Elsevier, New York.

Morrow, C. A., D. E. Moore, and D. A. Lockner (2000), The effect of mineral bond strength and adsorbed water on fault gouge frictional strength, *Geophys. Res. Lett.*, *27*, 815–818.

Pytte, A. M., and R. C. Reynolds (1989), The thermal transition of smectite to illite, in *Thermal History of Sedimentary Basins: Methods and Case Studies*, edited by N. D. Naeser and T. H. McCulloch, pp. 33–40, Springer, New York.

Saffer, D. M., and C. Marone (2003), Comparison of smectite- and illite-rich gouge frictional properties: Application to the updip limit of the seismogenic zone along subduction megathrusts, *Earth Planet. Sci. Lett.*, *215*, 219–235.

Saffer, D. M., K. M. Frye, C. Marone, and K. Mair (2001), Laboratory results indicating complex and potentially unstable frictional behavior of smectite clay, *Geophys. Res. Lett.*, *28*, 2297–2300.

Scholz, C. H. (2002), *The Mechanics of Earthquakes and Faulting*, 2nd ed., Cambridge Univ. Press, New York.

Underwood, M. B. (2007), Sediment inputs to subduction zones: Why lithostratigraphy and clay mineralogy matter, in *The Seismogenic Zone of Subduction Thrust Faults*, edited by T. Dixon et al., Columbia Univ. Press, New York.

Vrolijk, P. (1990), On the mechanical role of smectite, *Geology*, *18*, 703–707.

Vrolijk, P., and B. A. van der Pluijm (1999), Clay gouge, *J. Struct. Geol.*, *21*, 1039–1048.

M. J. Ikari, C. Marone, and D. M. Saffer, Department of Geosciences, Pennsylvania State University, 536 Deike Bldg., University Park, PA 16802, USA. (mikari@geosc.psu.edu)